



# Hypoxia is common in temperate headwaters and driven by hydrological extremes

Jacob S. Diamond<sup>a,\*</sup>, Florentina Moatar<sup>a</sup>, Rémi Recoura-Massaquant<sup>a</sup>, Arnaud Chaumot<sup>a</sup>, Jay Zarnetske<sup>b</sup>, Laurent Valette<sup>a</sup>, Gilles Pinay<sup>c</sup>

<sup>a</sup> RiverLy, INRAE, Centre de Lyon-Grenoble Auvergne-Rhône-Alpes, 69100, France

<sup>b</sup> Department of Earth and Environmental Sciences, Michigan State University, East Lansing, MI, USA

<sup>c</sup> Environnement, Ville & Société (EVS UMR5600), Centre National de la Recherche Scientifique (CNRS), Lyon, France

## ARTICLE INFO

### Keywords:

Drought  
Hypoxic  
Drying  
Storms  
Rewetting  
Dissolved oxygen  
Temperature

## ABSTRACT

Hypoxia, or dissolved oxygen (DO) at low enough levels to impair organisms, is a particularly useful indicator of the health of freshwater ecosystems. However, due to limited sampling in headwater networks, the degree, distribution, and timing of hypoxia events are not known across the vast majority of most river networks. We thus sought to clarify the extent of hypoxia in headwater networks through three years of instrumentation of 78 sites across eight temperate, agricultural watersheds. We observed broadly distributed hypoxia, occurring 4 % of the time across 51 of the 78 sites over 20 months. The hypoxia was driven by three mechanisms: storm events, drying, and rewetting, with drying as the most common driver of hypoxia (55 % of all hypoxic event types). Drying induced hypoxia was most severe in smaller streams (Strahler orders  $\leq 3$ ), whereas storm events preferentially induced hypoxia in the larger streams (Strahler orders 3–5). A large diversity in DO trajectories towards hypoxia depended on hydrologic event type, with subsequent expected differences in mortality profiles of a sensitive species. Predictive models showed the most vulnerable sites to hypoxia were small streams with low slope, particularly during hot, low discharge periods. Despite variation among hypoxic events, there was remarkable similarity in the rate of DO drawdown during hypoxia events (ca.  $1 \text{ mg O}_2 \text{ L}^{-1} \text{ d}^{-1}$ ). This drawdown similarity may be a useful rule-of-thumb for managers, and we hypothesize that it is either a signal of increasing lateral inflow of low DO water or a signal of increasing downstream oxygen demand. Overall, we posit that hypoxia is likely a common feature of most headwater networks that often goes undetected. Headwater hypoxia may become more common under increasingly dry conditions associated with climate and water resource management changes, with important implications for biological communities and biogeochemical processes.

## 1. Introduction

Low oxygen concentrations in fresh and salt waters are common and increasing in both spatial and temporal extent around the world (Breitburg et al., 2018; Jenny et al., 2016). While mechanisms driving low oxygen concentrations, or hypoxia, are well documented in lakes and coastal areas, it is less well documented or understood in river networks that are often assumed to be oxic. Hypoxia is known to lead to mortality (Rabalais et al., 2010 and references therein), mobilize chemically reduced contaminants into the water column (Saup et al., 2017), and exacerbate greenhouse gas emissions (Bastviken et al., 2004). Sparked both by these growing environmental concerns and by a proliferation of rather inexpensive, accurate, and rugged dissolved

oxygen sensor technology (Rode et al., 2016), interest is mounting to understand the spatiotemporal distributions of hypoxia in river waters (Dutton et al., 2018; Garvey et al., 2007). Yet, of these river systems, headwater stream hypoxia dynamics are still the least understood (Błaszczak et al., 2019; Carter et al., 2021; Gómez-Gener et al., 2020; Pardo and García, 2016).

Hypoxia in river systems can arise from a number of interacting processes linked to high levels of respiratory or reductive processes somewhere in the hydrologic network. Broadly speaking, we can define five underlying drivers of hypoxia, each of which is associated with a dominance of respiratory processes in the oxygen budget. In no particular order, there are: 1) excess N and P input leading to eutrophication, particularly in lakes/estuaries (Breitburg et al., 2018; Smith and

\* Corresponding author at: RiverLy, INRAE, 5 rue de la Doua, Villeurbanne, 69100, France.

E-mail address: [jacob.diamond@inrae.fr](mailto:jacob.diamond@inrae.fr) (J.S. Diamond).

<https://doi.org/10.1016/j.ecolind.2023.109987>

Received 27 November 2022; Received in revised form 12 January 2023; Accepted 4 February 2023

Available online 10 February 2023

1470-160X/© 2023 The Author(s). Published by Elsevier Ltd. This is an open access article under the CC BY-NC-ND license (<http://creativecommons.org/licenses/by-nc-nd/4.0/>).

Schindler, 2009), 2) point source pollution (Mallin et al., 2006; McConnell, 1980), 3) storms, which can bring in low O<sub>2</sub> groundwater (Carter et al., 2021) or oxygen demanding substances (Dutton et al., 2018; Kerr et al., 2013; Whitworth et al., 2012), 4) drying (Pardo and García, 2016; Tramer, 1977), and 5) rewetting, which may stimulate microbial activity (Acuña et al., 2005). These varied drivers, in particular storms, drying, and rewetting, may have distinct hypoxic signatures that are important for the survival of biota.

The low primary productivity relative to respiratory processes (Diamond et al., 2021; Vannote et al., 1980) and increased likelihood for drying of headwater streams (Godsey and Kirchner, 2014) suggests their trends towards longer and more frequent hypoxia events. Still, most studies on stream hypoxia focus on humid climate streams and rivers larger than Strahler order 2; less is known regarding the smaller order streams of headwater networks (Bishop et al., 2008) that typically experience greater flow intermittence (Gómez-Gener et al., 2020). These headwaters are the network capillaries connecting land to the river network and they physically dominate total stream length and benthic

area of river networks (Benstead and Leigh, 2012; Strahler, 1957). By not studying this dominant portion of river networks, there may be a large underestimation of the total extent of freshwater hypoxia.

Hypoxic episodes may become more common in headwaters under increased climate-driven drought frequency and intensity (Dai, 2013; Samaniego et al., 2018), especially in agricultural areas already experiencing irrigation-induced water deficits (Elliott et al., 2014). The link between hydrologic extremes and hypoxia further suggests that headwaters may exhibit disproportionately more hypoxia than downstream reaches, as they typically have greater hydrologic responses to climate and land use change (Penn et al., 2016). Moreover, small stream drying patterns typically lead to a predictable series of increasingly disconnected aquatic states (Stanley et al., 1997; Gallart et al. 2012; Godsey and Kirchner, 2014) with understudied effects on subsequent heterogeneity in oxygen. Importantly, hypoxia and its spatiotemporal heterogeneity likely plays an important, but as of yet unknown role in community physiological effects and species mortality.

We addressed these research gaps by studying the oxygen regimes in

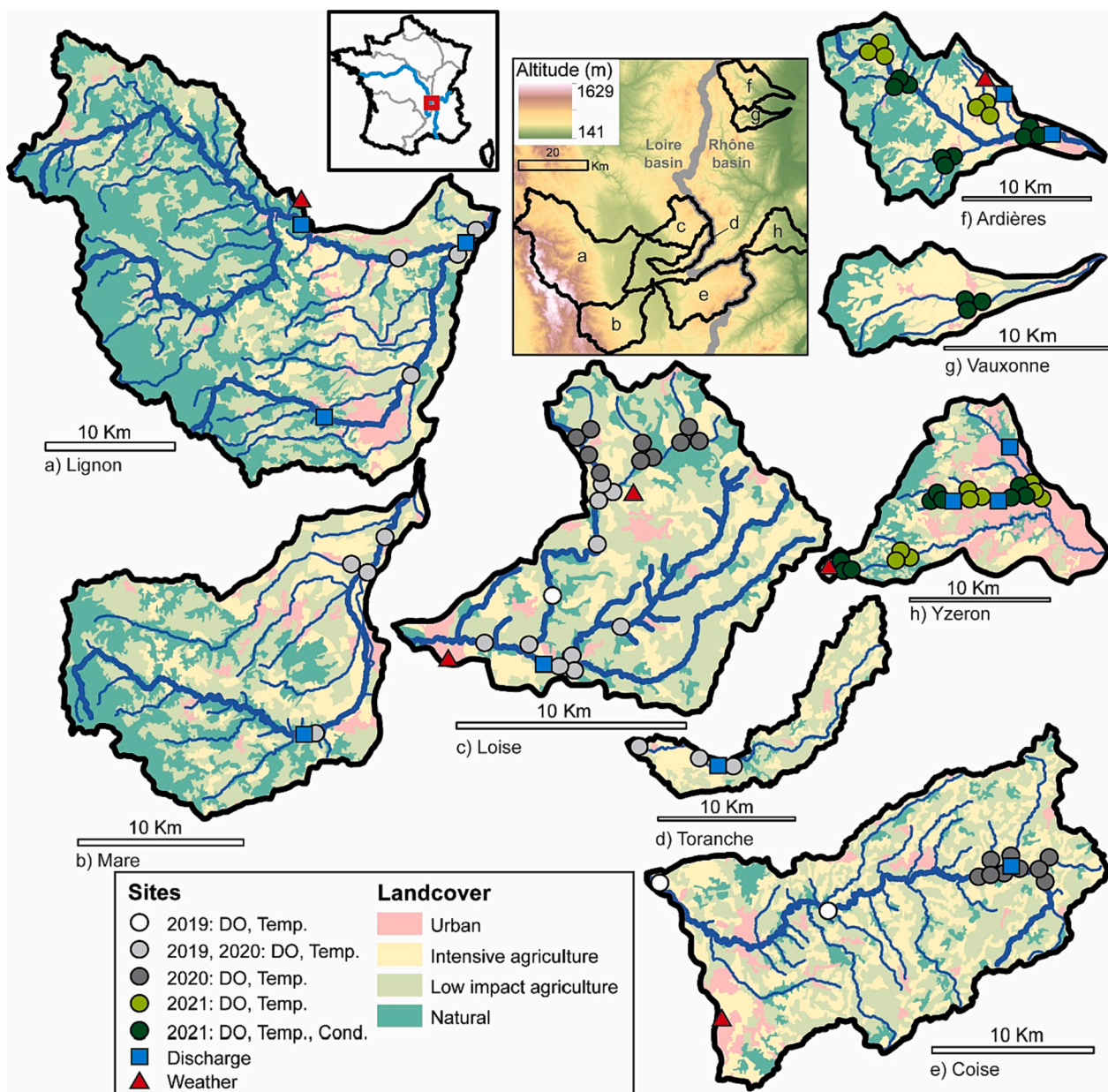


Fig. 1. Map of instrumented study sites with points indicating sensor placement and monitoring duration.

agricultural headwater rivers to assess the environmental conditions leading to headwater hypoxia, and the subsequent degree of hypoxia throughout the networks. We hypothesized that hypoxic events would arise under drying, storm, and rewetting conditions, but that hypoxia would be greatest and most common in the smallest streams due to their increased risk for drying and pooling. We further evaluated the potential impact of hypoxia on aquatic animal communities using the modeled mortality response of the amphipod *Gammarus fossarum*, a sentinel organism of water quality in stream ecosystems (Chaumot et al., 2015; Kunz et al., 2010) known for its sensitivity to dissolved oxygen (Hervant and Mathieu, 1995; Maltby, 1995; Meijering, 1991). We hypothesized that the model organisms would exhibit a mortality threshold response to lower DO, which we could use as a way to set an ecologically relevant definition of hypoxia in our stream networks.

## 2. Methods

### 2.1. Study area

We instrumented 78 sites, spanning Strahler orders 1–5 across eight catchments in France: 1) Coise, 2) Loire, 3) Toranche, 4) Mare, 5) Lignon, 6) Ardières, 7) Vauxonne, and 8) Yzeron (Fig. 1, Table 1). We monitored these catchments monitored for hypoxia from 3 July 2019 to 15 October 2021 (except winters from November 1–February 28). Overall, we sampled 6, 14, 29, 21, and 8 sites in Strahler orders 1–5, respectively. All sites are predominately shaded in the growing season (May–September) by riparian trees (Diamond et al., 2021; Diamond et al., 2022), and aquatic primary production is dominated by benthic algae that experience maximal productivity in April just before riparian leaf-out (Diamond et al., 2021). Indeed, these headwater sites are heterotrophic, with ecosystem respiration (ca.  $-3 \text{ g O}_2 \text{ m}^{-2} \text{ d}^{-1}$ ) generally an order of magnitude greater than gross primary productivity (ca.  $0.3 \text{ g O}_2 \text{ m}^{-2} \text{ d}^{-1}$ ; Diamond et al., 2021).

The first five catchments (Coise–Lignon) are primarily agricultural headwater catchments of the Loire River basin, and were instrumented from July 2019–October 2020, with 4, 11, 15, 8, and 3 sites in orders 1–5, respectively. In these catchments, granite and gneiss lithology at upper catchment boundaries gradually gives way to thick alluvium with clay and sand at catchment outlets in a flat basin known as the Forez plain. The geology in the upper reaches prevents substantial aquifer storage leading to regular drying. Topography is characterised by rolling hills with successions of plateaus separated by steep slopes. Climate in these catchments is continental, with mean annual temperature of  $11 \text{ }^\circ\text{C}$  (range during measurement period =  $0.0\text{--}34.3 \text{ }^\circ\text{C}$ ) and mean annual precipitation of 800 mm.

The Ardières and Vauxonne catchments are adjacent, but just across the regional drainage divide and are tributaries of the Saône River, which itself is a tributary of the Rhône River. From 8 March 2021 to 14 October 2021, we instrumented 2, 6, 8, and 3 sites of Strahler order 2, 3, 4, and 5 respectively. These two catchments drain a hilly landscape of vineyards (32 % land cover) exposed to pesticides (Montuelle et al., 2010). Soil is sandy loam on a shallow Hercynian crystalline bedrock. Climate is temperate with a mean annual air temperature of  $17.1 \text{ }^\circ\text{C}$  ( $-2.1\text{--}35.2 \text{ }^\circ\text{C}$ ) and mean annual precipitation is 940 mm, with intense summer thunderstorms. The combination of climate, soil and steep slopes (up to  $>30 \%$ ) is conducive to infiltration and sub-surface lateral flow (Gouy et al., 2021).

The last catchment, the Yzeron, is a direct tributary of the Rhône River, draining a steep agricultural and forested landscape composed of magmatic and metamorphic (granite, gneiss, schist) bedrock that leads downstream to a semi-urban/urban zone with Quaternary fluvio-glacial and glacial deposits. From 08 March 2021 to 15 October 2021, we instrumented 2, 3, 6, 6, and 1 sites from Strahler orders 1–5, respectively. The climate is a mix of continental/Mediterranean with mean annual temperature  $13.8 \text{ }^\circ\text{C}$  ( $-5.5\text{--}28.1 \text{ }^\circ\text{C}$ ) and mean annual rainfall 800 mm (Gnouma, 2006), which predominately occurs in spring and autumn. The hydrological regime is pluvial with low flows in summer and floods in autumn and spring. Road and storm sewages designed for flood mitigation allow rapid transport of urban runoff to downstream channels of the Yzeron.

### 2.2. Data collection and processing

We monitored the sites for dissolved oxygen (DO;  $\text{mg L}^{-1}$ ) and stream temperature ( $^\circ\text{C}$ ) for variable periods between July 2019 and October 2021, but not during winter (November – February; Fig. 1). At each site, DO and stream temperature were measured every 15 min with an in-situ sensor (HOBO U26-001, Onset Computer Corporation, Massachusetts, USA) instrumented with a copper anti-biofouling guard. At 12 sites in 2020 and 18 sites in 2021, we installed conductivity sensors (HOBO U24-001, Onset Computer Corporation, Massachusetts, USA). We cleaned DO and conductivity sensors with a toothbrush every two weeks to remove biofouling. Prior to deployment, we lab-calibrated DO sensors with both 100 % water-saturated air and with sodium sulphite for 0 % saturation. Conductivity sensors were calibrated based on field measurements obtained with a calibrated handheld probe (Pro Plus, YSI Inc., Ohio, USA) at the beginning and end of each two-week measurement period per manufacturer instructions. We also measured DO and temperature with the calibrated handheld probe at each field visit to check for sensor drift and develop corrections as needed. We

**Table 1**

Characteristics of the Loire and Rhône tributaries' catchments and summary of their hydrochemistry from grab samples, mean  $\pm$  sd (n).

| Variable   | Loire                |                      |                     |                      |                      | Rhône                        |                    |                      |
|--|----------------------|----------------------|---------------------|----------------------|----------------------|------------------------------|--------------------|----------------------|
|  | Coise                | Loire                | Toranche            | Mare                 | Lignon               | Ardières                     | Vauxonne           | Yzeron               |
| N sites  | 11                   | 20                   | 3                   | 4                    | 4                    | 15                           | 3                  | 18                   |
| Area ( $\text{km}^2$ )                             | 6.1–350              | 0.8–132              | 54.7–76.1           | 61.9–233             | 62.1–664             | 3.6–142                      | 6.6–46.0           | 0.8–59.4             |
| Alt. (m)   | 344–619              | 337–627              | 338–377             | 352–422              | 330–360              | 199–389                      | 227–228            | 197–731              |
| Q* ( $\text{m}^3 \text{ s}^{-1}$ )                 | 0.17                 | 0.13                 | 0.06                | 0.34                 | 1.11                 | 0.59                         | 0.19               | 0.10                 |
| pH   | $7.8 \pm 0.2$ (40)   | $7.5 \pm 0.4$ (123)  | $7.7 \pm 0.4$ (27)  | $7.8 \pm 0.2$ (35)   | $7.6 \pm 0.3$ (43)   | $7.5 \pm 0.1$ (91)           | $7.8 \pm 0.1$ (17) | $7.6 \pm 0.3$ (107)  |
| SpC** ( $\mu\text{S cm}^{-1}$ )                    | $296 \pm 129$ (71)   | $315 \pm 255$ (156)  | $320 \pm 82$ (33)   | $193 \pm 79$ (49)    | $136 \pm 57$ (59)    | $145 \pm 45$ (166)           | $238 \pm 59$ (32)  | $322 \pm 124$ (195)  |
| DOC†† ( $\text{mg L}^{-1}$ )                       | $4.6 \pm 1.1$ (24)   | $4.3 \pm 1.6$ (73)   | $7.0 \pm 1.4$ (13)  | $7.0 \pm 1.6$ (20)   | $5.1 \pm 1.6$ (26)   | $3.3 \pm 0.9$ (125)          | ND                 | $6.7 \pm 2.9$ (78)   |
| $\text{NO}_3\text{-N}$ ( $\text{mg L}^{-1}$ )      | $2.3 \pm 1.9$ (24)   | $2.2 \pm 2.1$ (73)   | $2.4 \pm 2.3$ (13)  | $1.2 \pm 0.6$ (20)   | $0.9 \pm 0.6$ (26)   | $2.2 \pm 1.8$ (88)           | $2.0 \pm 1.6$ (17) | $2.1 \pm 1.3$ (78)   |
| $\text{PO}_4^{3-}\text{-P}$ ( $\text{mg L}^{-1}$ ) | $0.12 \pm 0.12$ (24) | $0.07 \pm 0.07$ (73) | $0.11 \pm 0.1$ (13) | $0.08 \pm 0.05$ (20) | $0.08 \pm 0.06$ (26) | $0.1 \pm 0.1^{\dagger}$ (45) | ND                 | $0.08 \pm 0.07$ (78) |

ND = no data.

Note: Overall, we sampled 6, 14, 29, 21, and 8 sites in Strahler orders 1–5, respectively.

† altitude in meters above NGF IGN69 datum.

\* interannual median at the outlet during sampling period.

\*\* specific conductance at  $25 \text{ }^\circ\text{C}$ .

†† dissolved organic carbon.

‡ estimated from Montuelle et al. (2010).

placed sensors in the middle of the water column, and as close to the thalweg as possible. As streams began to dry, we vertically repositioned sensors to keep them submerged and continuously capture stream DO and prevent loss of data.

Across all sites, we measured DO and stream temperature at 15-minute intervals for a total of 1,687,776 measurements. The quality controls applied to all DO data prior to analysis are described in detail in [Diamond et al. \(2021\)](#). Briefly, we 1) averaged 15-minute data to hourly resolution to reduce file sizes and processing time, 2) removed data that were extremely noisy, collected in dry conditions, or otherwise of suspect quality, and 3) corrected for minimal sensor drift. For data that passed quality control ( $n_{DO} = 380,161$ ), we calculated hourly DO saturation ( $DO_{sat}$ ) and specific conductance.

### 2.3. Storm, drying, and rewetting events

We observed three environmental events conducive to hypoxia across our sites: 1) storms, 2) drying, and 3) rewetting. Each of these environmental events were identified according to the following definitions. First, we classified storm events as a doubling of baseflow ([Carter et al., 2021](#)), with storms at least 24 h apart counting as separate events. We used the functions *high.spells* and *baseflow* (based on a Lyne-Hollick recursive digital filter) from the *hydrostats* R package ([Bond, 2022](#)) to determine these events. Through sensitivity analyses, we determined these criteria to accurately and reproducibly capture each distinct event in the observed discharge time series. To determine storm effects on DO, we examined the three days before the storm peak flow and the week following the peak flow ([Carter et al., 2021](#)).

Second, to classify distinct drying events, we relied on a combination of sensor data, field observations, and discharge data. Ideally, accurate local discharge or stage data should characterize these events, but the large number of sites precluded continuous measurement at each location, and there is a well-known problem with low-flow accuracy from local stream network gages ([Zimmer et al., 2020](#)). Hence, to indicate dry periods, we used the observation that DO sensors read near-saturation and experience air-temperature-like fluctuations when they are out of the water. These dry-period DO sensor observations are directly supported by 1) concurrent conductivity measurements (reading near  $0 \mu S cm^{-1}$ ), 2) field observations of dry stream beds, and 3) near-zero or zero-flow measurements of discharge at local discharge stations. Therefore, these moments (i.e., when sensors are out-of-water) represent the end-points of our drying periods. We then determined the beginning points of our drying periods by extending the end-point backwards in time to a point when specific discharge measurements exceeded the 10 % percentile, using the *low.spell.lengths* function from *hydrostats*.

Third, rewetting events were demarcated by typically rapid and large reductions in temperature, and increases in conductivity of stream water after dry periods. These moments were also associated with measured rainfall events and concomitant discharge responses, so we have high confidence in the start time of rewetting events. The length of a rewetting event lasted either until the stream dried again (see above), or until discharge exceeded the 10 % percentile. To avoid over-counting drying events, we did not consider the drying after rewetting to be a drying event as defined above unless the discharge exceeded the 10 % percentile before re-drying after rewetting. For all hydrologic events (storms, drying, and rewetting), we assumed that all sites within a watershed behaved synchronously and with the same specific discharge ([Diamond et al., 2022](#)).

### 2.4. Hypoxia evaluation

In this study, we defined instantaneous hypoxia conditions to occur in the stream water when DO is  $<3 mg O_2 L^{-1}$ . This instantaneous hypoxia level was selected for three primary reasons: 1) it is national threshold value for “bad” ecological potential of water quality in France ([Ministère chargé de l’écologie, 2019](#)), 2) it appears to be a threshold for

mortality in the biological indicator species, *Gammarus fossarum* ([Fig. S1](#)), and 3) measurements of DO concentrations are less uncertain and require fewer assumptions than estimates of DO percentage saturation, although this metric is still commonly used (e.g. 50 %, [Carter et al., 2021](#)). Some regulatory agencies define coastal hypoxia as  $<2 mg L^{-1}$  ([NSTC, 2003](#)) though evidence suggests freshwater biota experience chronic toxicity below  $5 mg L^{-1}$  ([Saari et al., 2018](#)). Overall, there is no single definition for hypoxia, and different numeric thresholds may be appropriate for the regulation or study of specific impacts (in  $mg L^{-1}$  or % saturation).

As there is no single assessment of hypoxia and its impacts, we evaluated the degree of hypoxia in several ways. Apart from simply calculating total hours and percentage of hypoxia within and across sites, we also delineated continuous hypoxic events (with up to a 2-hour gap of  $DO >3 mg L^{-1}$ ), taking into account their lengths, and periodicity, and the diel distributions of hypoxia. We further calculated rates of DO drawdown leading to hypoxia during storm, drying, and rewetting events by fitting linear regressions through daily minima ([Carter et al., 2020](#)). Finally, we attempted to identify simple predictors of hourly hypoxia (i.e., binary: hypoxic or oxic) with logistic regression and classification trees (R package *rpart*; [Therneau and Atkinson, 2022](#)). Potential predictors of DO conditions measured included stream habitat of the DO sensor (pool, riffle, or run; visually assessed), hourly stream temperature, daily specific discharge of the catchment, reach slope, Strahler order, distance from the source, and altitude. Data were highly skewed towards oxic conditions, so we balanced the data with combined over- and under-sampling using the R package *ROSE* ([Lunardon et al., 2014](#)). We split the dataset into training (70 %) and testing (30 %) data for model building and validation, respectively.

### 2.5. Prediction of gammarid mortality during hypoxic events

To connect observed hypoxia events with hypoxia physiological response for stream biota, we modeled *Gammarus fossarum* (“gammarid”) mortality using measured DO concentrations from contrasting hypoxic event types. We chose gammarids as an indicator species because they constitute the dominant macroinvertebrate biomass in many European headwaters ([MacNeil et al., 1997](#)) and are a key functional species as both detritivores and as a dominant food source for secondary consumers. Hence, gammarid mortality response to spatio-temporal variation hypoxia is a useful indicator of how overall live ecosystem biomass and turnover rates may change under varying oxygen levels.

We used the in-situ measured DO concentrations as input to a General Unified Threshold model of Survival (GUTS) ([Jager et al., 2011](#)). The GUTS toxicokinetic-toxicodynamic model, based on bioassay survival data, is regularly used in prospective hazard assessment of pesticides and fluctuating concentrations of toxic chemicals ([Ockleford et al., 2018](#)). GUTS quantifies mortality rate evolution based on the internal concentrations of hazardous compounds in organisms, which are controlled both by uptake rates and internal contaminant elimination rates ([Baudrot et al., 2018](#)). We adapted GUTS to include hypoxic stress instead of toxic stress by considering the DO deficit below an arbitrary value of  $12 mg L^{-1}$  as the stressor input metric (instead of contaminant concentration). Using the web-interface MOSAIC (<https://mosaic.univ-lyon1.fr/guts>) ([Charles et al., 2018](#)), we calibrated the GUTS model with an experimental dataset of gammarid mortality in laboratory conditions under different constant levels of DO deficit ([Recoura-Masquand et al., 2022](#)). We used the reduced individual tolerance version of the model (GUTS-RED-IT), which assumes a log-logistic distribution of sensitivity threshold among individuals. The calibration experiment consisted of monitoring mortality over a five-day laboratory exposure of 300 male organisms of homogenous body size ( $\sim 10 mm$ ) to 10 constant nominal DO concentration conditions (8, 6, 5, 4, 3.5, 3, 2.5, 2, 1.5 and  $1 mg L^{-1}$ , respectively), with three replicates of 10 individuals per concentration condition ([Fig. S1](#)). DO deficits were obtained by bubbling  $N_2$

gas through water columns. All detailed experimental data are available from the open access data repository Recherche Data Gouv (Recourant-Massaquant et al. 2022). We then used the calibrated GUTS-RED-IT model to estimate potential mortality responses under observed hypoxic scenarios from three storm events and five drying events.

### 3. Results

#### 3.1. Degree of hypoxia across sites

Overall, we observed 16,781 h of hypoxia ( $DO < 3 \text{ mg L}^{-1}$ ), an average of 4.4 % of all site hourly measurements from 2019 to 2021. Hypoxia occurred at 51 of 78 sites for at least one hour of hypoxia, and at 37 sites for at least 1 % of the time. The greatest degree of hypoxia was in 2019, accounting for 9.2 % of all measurements that year, followed by 2020 with 6.2 %, and 2021 with 1.3 %. Note that in 2021, in addition to being a wetter year (Fig. 2b), the sites changed from the Loire to the Rhône basin (Fig. 1). Among catchments, the Toranche experienced the most hypoxia (12.9 % or 2,335 h), and the Vauxonne the least (0.3 % or 57 h; Table S1). In general, hypoxia was spatially heterogeneous, but drying tended to synchronize hypoxia within catchments. For example, in late July 20, when most sites in the Loise catchment were almost dry,

sites ranging 4.2–31.4  $\text{km}^2$  (7 out of 16 sites) exhibited hypoxia at the same time before drying.

Across our sites, we observed correlations between the degree of monthly hypoxia and stream temperature (Fig. 2a) and specific discharge (Fig. 2b). Hence, hypoxia was greatest in summer months (Fig. 2d) when temperatures were greatest and discharge was lowest. There were negligible differences in hypoxia rates between night and day, although solar noon was the least likely time to observe hypoxia (Fig. 2c). Mean hypoxic duration was 10 h, and while this did not vary over time (Fig. 2d), there was two orders of magnitude variation across events (range = 1–210 h). In general, differences in degree of hypoxia among Strahler orders were marginal (Table 2), and did not correspond to downstream trends ( $p > 0.05$  for all linear fits). Still, Strahler order 1 exhibited the lowest degree of hypoxia for all metrics. Across the hydrologic drivers, hourly hypoxia occurred 54 % in storms, 9 % in drying, and 38 % in rewetting events.

#### 3.2. Storm events

We recorded 152 storm events across the 13 discharge gages with an average storm pulse length of  $2.6 \pm 4.2$  days (mean  $\pm$  sd; range = 1 h–22.1 days), leading to 776 site-events. Of those site-events, 107

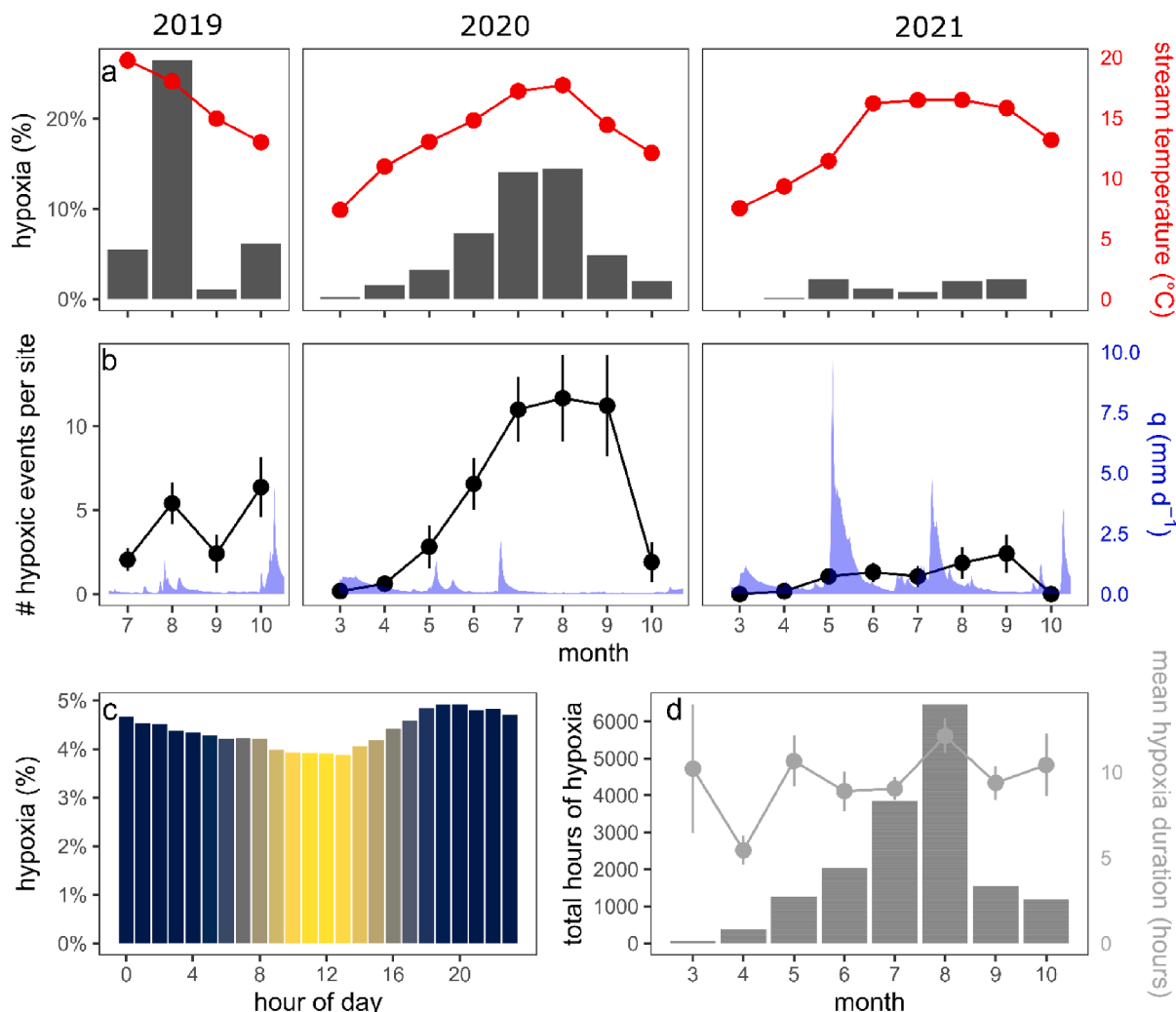


**Fig. 2.** Time series of hypoxia metrics. a) Monthly percentage of measurements that were hypoxic (bars) with mean monthly across-site stream temperature (red) for 2019–2021 (columns for a and b). b) Mean monthly number of unique hypoxic events across sites (black, vertical bars are standard errors) and mean daily specific discharge (blue) across gaging stations. c) Hourly percentage of measurements that were hypoxic across sites and years, with lighter colors indicating daylight hours. d) Total hours of hypoxia (bars) and the mean duration of hypoxia (grey, vertical bars are standard errors) across sites and years by month. (For interpretation of the references to colour in this figure legend, the reader is referred to the web version of this article.)

**Table 2**  
Hypoxia summary statistics by Strahler order, mean ± sd when given.

| Strahler order | Total hypoxia (hours) | Percentage of time hypoxic* (%) | Unique hypoxia events** (n) | Event length† (hours) | Time between events‡ (days) | Night hypoxia‡ (%) |
|----------------|-----------------------|---------------------------------|-----------------------------|-----------------------|-----------------------------|--------------------|
| 1              | 786                   | 3.1                             | 34                          | 8±6                   | 3.0±11.3                    | 51 %               |
| 2              | 3180                  | 4.9                             | 44                          | 9±11                  | 5.5±18.8                    | 49 %               |
| 3              | 7778                  | 5.1                             | 73                          | 10±13                 | 9.3±43.1                    | 48 %               |
| 4              | 3015                  | 3.0                             | 37                          | 10±10                 | 13.7±45                     | 49 %               |
| 5              | 2022                  | 5.6                             | 27                          | 14±17                 | 9.9±31.5                    | 50 %               |

\* Total hours of hypoxia divided by total hours of DO measurements × 100.

\*\* Event defined as at least one hour of DO < 3 mg L<sup>-1</sup>; events continue with up to 2-hour gap in hypoxia.

† Event length begins at time of first hypoxia and continues until hypoxia ends, with up to 2-hour gap in hypoxia.

‡ The time between hypoxic events.

‡ The percentage of total hypoxia that was measured at night, where night is defined as <200 μmol m<sup>-2</sup> s<sup>-1</sup> PAR.

resulted in at least one hour of hypoxia. For 131 of the 669 site-events without hypoxia, there was no change in DO mean or variance after the storm peak (ANOVA and t-tests of 5 days before and after;  $p > 0.01$ ), whereas 414 of them exhibited an increase in DO, but no change in DO diel range. Storm events resulting in hypoxia occurred predominately in higher order sites, with 87 % in orders 3–5, and 62 % in orders 4–5. Storm events were the most common hydrologic driver of hypoxia, accounting for 47 % of all hypoxic events.

DO trajectories following storm events were highly variable

(Fig. S2). Of the storms that induced hypoxia, it took a median of 41 h (53±48 h) after peak discharge to become hypoxic, ignoring sites that were hypoxic prior to the storm. This is the amount of time for DO to drop between 8.0 and 3.3 mg L<sup>-1</sup> when using the median and mean rates of DO decrease (Fig. 3b). Sites stayed hypoxic for a median of 7 h (20 ±32 h) after first becoming hypoxic. There were 48 events where peak discharge rapidly induced oxic conditions to previously hypoxic sites, but oxic conditions rarely lasted for more than a few days (Fig. 3a). These event types were spread across 25 sites and every Strahler order

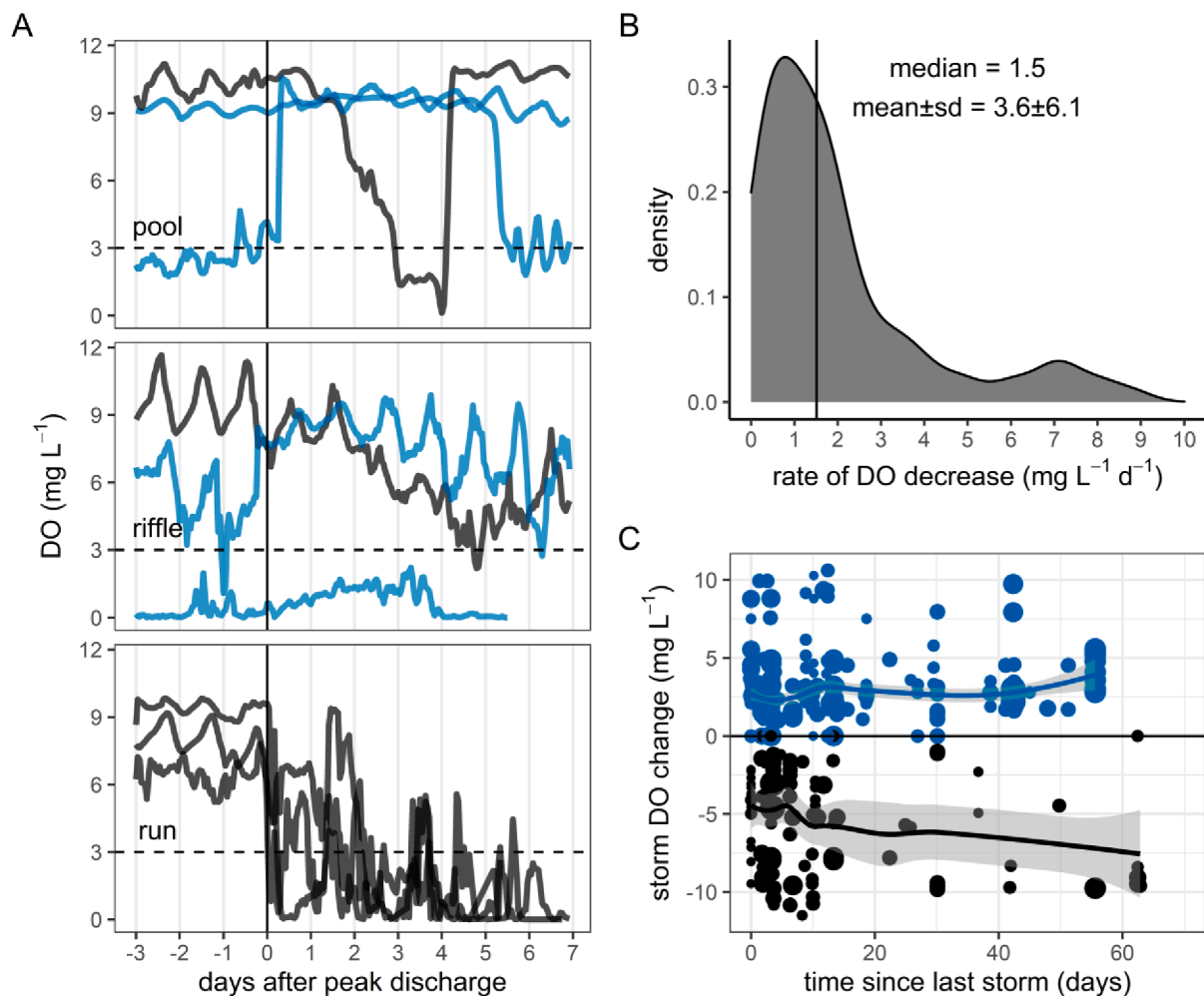


**Fig. 3.** Summary of storm event effects on DO. A) three different storm events for each of three different habitat types (pool, riffle, run) with colors indicating whether DO increased (blue) or decreased (black) after the storm event. Dashed line indicates hypoxia and vertical line indicates peak discharge. B) Distribution of DO decreases (black events in panel A) across all events that led to a decrease in DO. C) Comparison of change in DO (colors as in A) as a function of time since the last storm, with the point size indicating the magnitude of the storm pulse. LOESS lines with 95% confidence intervals are shown. (For interpretation of the references to colour in this figure legend, the reader is referred to the web version of this article.)

and habitat. Moreover, event types varied within sites, with no clear consistency in site-level DO response to storms. There were few obvious predictors of the effect of a particular storm event on changes to DO, with time since last storm event, baseflow before storm event, and storm pulse magnitude having no predictive power (Fig. 3c).

### 3.3. Drying

Across all 13 stream gages in the study area, dry conditions were recorded 86 times with a mean dry duration of  $6.7 \pm 11.2$  days (range = 8 h – 86 days). Flow was lowest in 2019 and 2020 (Fig. 2b). In the Loire basin, the Loire, Coise, and Toranche catchments experienced zero-flow for 2 %, 2 %, and 24 % of days in 2019, and 11 %, 11 %, 29 % in 2020. Average dry durations for those catchments were 1, 1, and 4.5 days in 2019, and 1, 1, and 80 days in 2020. In the Rhône basin, sites in the Yzeron catchment in 2021 also experienced drying 1.5–4.6 % of the time, with average site dry durations of 4.9–11.8 days. Using our criteria to determine if a sampling site was dry, we estimate that 23 of 78 sites became dry at least once. Within those 23 sites, we observed 60 distinct drying events ( $2.6 \pm 1.5$  events per site). The remaining results refer to these hypoxic drying events (Fig. 2a).

Drying was the second most common hydrologic driver of hypoxia, accounting for 30 % of all hypoxic events. The mean hypoxia duration during drying was 6.2 h (range = 1–55 h); the greatest durations occurred in Strahler order 2 (mean =  $9.3 \pm 9.5$  h). The smaller Strahler orders (1–3) were twice as likely to become hypoxic during drying than to remain oxic, and for Strahler order 1 drying events always resulted in hypoxia. The mean decrease in daily DO minima was  $1.3 \text{ mg L}^{-1} \text{ d}^{-1}$  (Fig. 4b), with relatively little variation (IQR = 0.6–1.5  $\text{mg L}^{-1} \text{ d}^{-1}$ ).

This decrease in DO was not concomitant with increases in stream temperature, which did not exhibit increasing trends with drying ( $p > 0.05$ ). Once drying began, it took  $3.8 \pm 2.9$  days for sites to become hypoxic (IQR = 1.8–4.8 days). We observed increases ( $p < 0.05$ ) in DO diel ranges over drying periods in 12 instances (18 % of hypoxic drying events), with a mean increase of  $0.7 \pm 0.5 \text{ mg L}^{-1} \text{ d}^{-1}$ . Apart from Strahler order (Fig. 4c), there were no clear predictors (i.e., number of previous drying events, stream habitat, drying rate) for a site to become hypoxic during drying or on how long it would stay hypoxic.

### 3.4. Rewetting

There were 314 rewetting events according to our criteria with 46 of these events leading to at least one hour of hypoxia. These events occurred across 27 of 78 sampling sites. There was a mean duration of  $6 \pm 13$  days of dry conditions before rewetting, and sites went through an average of  $4.9 \pm 4.7$  drying and rewetting cycles. Rewetting led to more decreases than increases in DO (Fig. 5b). When only considering negative changes, the mean decrease in DO was  $-1.0 \pm 1 \text{ mg L}^{-1} \text{ d}^{-1}$  (median =  $-0.7 \text{ mg L}^{-1} \text{ d}^{-1}$ ). Apart from the fact that there were no riffle rewetting events that led to hypoxia (Fig. 5a), there were no other obvious controls on DO changes after rewetting, i.e., stream habitat, magnitude of increased discharge, dry period duration, or previous number of dry periods before rewetting (Fig. 5c).

### 3.5. Predicting hypoxia

A classification tree was able to predict instances of hypoxia across a training dataset with an accuracy of 81 % (c-statistic = 0.79, sensitivity

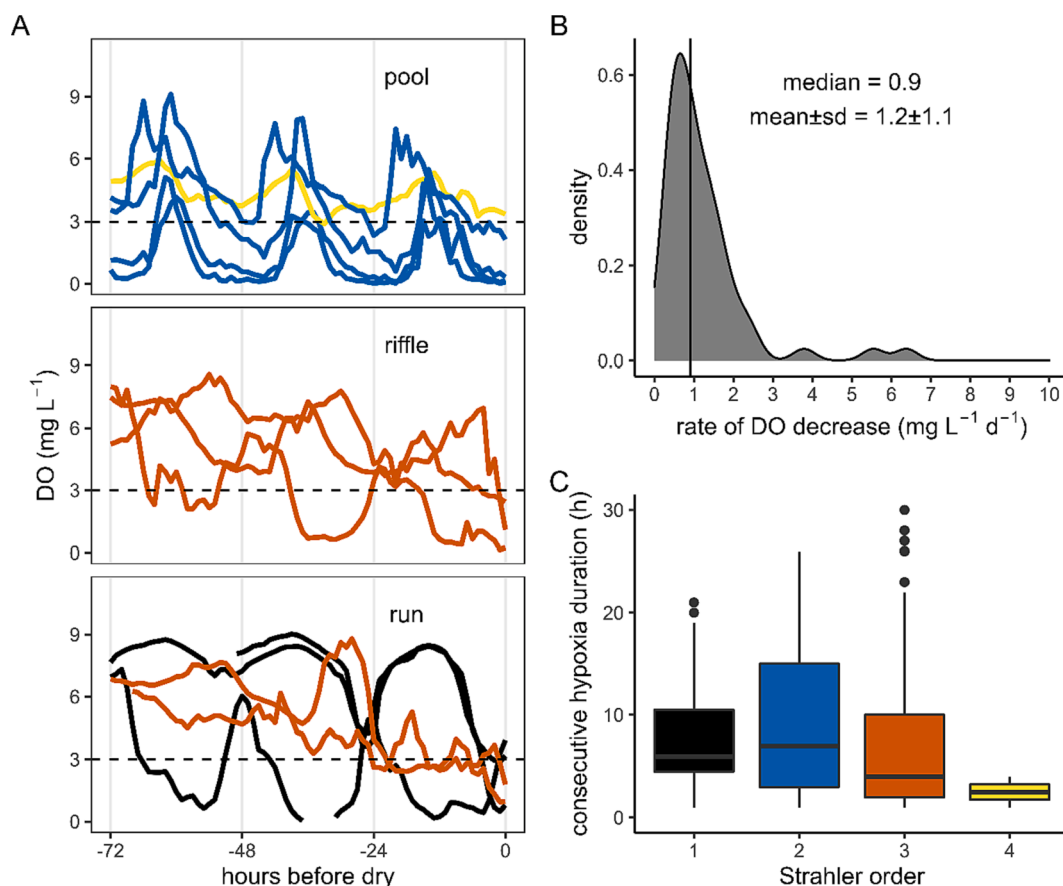
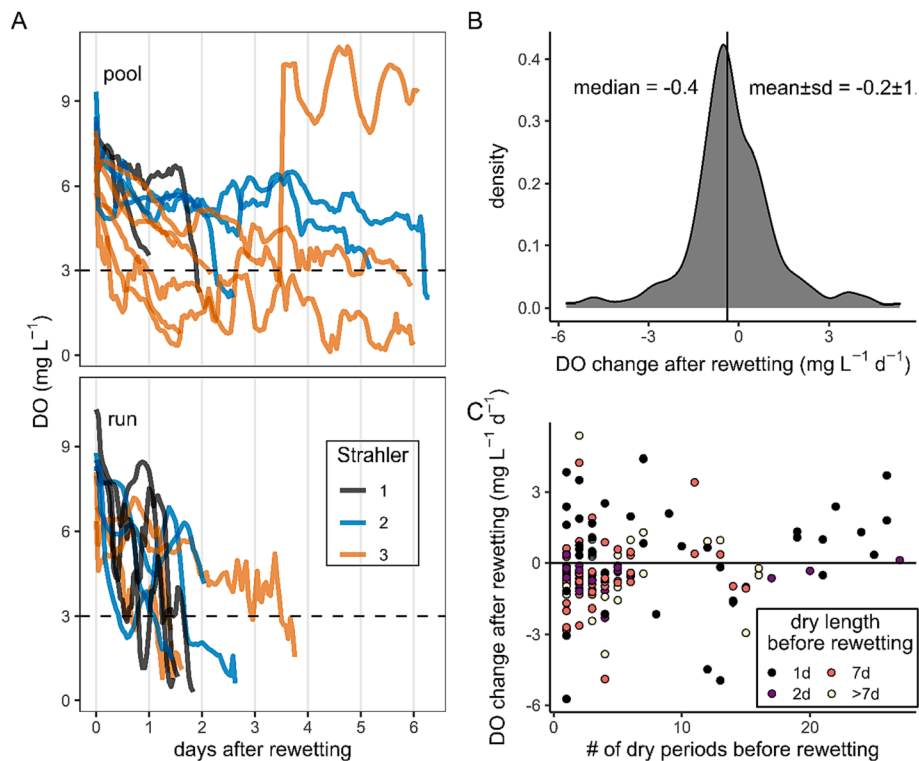


Fig. 4. Summary of drying hypoxia events. A) Three-to-four different drying events for each of three different habitat types (pool, riffle, run) with colors indicating Strahler order; dashed line indicates hypoxia. B) Distribution of DO decreases across all events. C) Length of consecutive hypoxia (colors as in A) as a function of Strahler order.



**Fig. 5.** Summary of rewetting event effects to DO. A) Different rewetting events leading to hypoxia for each of two different habitat types (pool and run; riffles did not experience rewetting hypoxia) with colors indicating Strahler order; dashed line indicates hypoxia. B) Distribution of DO changes across all events, vertical line indicates median. C) DO change after rewetting as a function of the number of dry periods before rewetting and the dry period duration (colors).

= 0.67, specificity = 0.82). Notably, the resulting 10-node tree predicted hypoxic events with probability = 0.79 for periods with stream temperature >11 °C, specific discharge <0.014 mm d<sup>-1</sup> (ca. 1–10 L s<sup>-1</sup> for these catchments), and Strahler order ≤3 (Fig. S3). The highest probability of hypoxia (p = 0.86) was observed for the same temperature conditions, but for discharge >0.014 mm d<sup>-1</sup>, and reach slopes 0.042–0.054 m m<sup>-1</sup>. The lowest probabilities for hypoxia were under cold-water conditions (temperature <11 °C) and high slope conditions (slope ≥0.054 m m<sup>-1</sup>). The variable importance for the classification tree were temperature = 34, slope = 32, specific discharge = 18, Strahler = 10, and habitat = 6. Similar variable importance was observed for a regression tree on DO (Fig. S4).

Given that discharge and temperature were the most important continuous variables in predicting hypoxia and DO at our sites, we used them as predictors in a logistic regression for hypoxia. The model (Table 3) performed relatively poorly (Fig. S5) with a pseudo R<sup>2</sup> = 0.10 (McFadden, 1987) and accuracy 63 % (c-statistic = 0.66, sensitivity = 0.69, and specificity = 0.63), especially when compared with the classification tree. Holding temperature constant, the odds of hypoxia decreased by 15 % for each unit increase in ln(q), whereas by holding discharge constant, the odds of hypoxia increased by 19 % for each °C increase.

**Table 3**  
Logistic regression results for probability of hypoxia.\*

| Coefficients | Estimate | SE   | z-value | p-value |
|--------------|----------|------|---------|---------|
| Intercept    | -3.0     | 0.02 | -151    | <0.0001 |
| ln(q)**      | -0.16    | 0.00 | -71     | <0.0001 |
| temperature  | 0.17     | 0.00 | -131    | <0.0001 |

\*  $\hat{p} = \frac{\exp(b_0 + b_1 \ln(q) + b_2 \text{temp})}{\exp(1 + b_0 + b_1 \ln(q) + b_2 \text{temp})}$   
 \*\* daily specific discharge [min d<sup>-1</sup>].

### 3.6. Gammarid mortality patterns

The laboratory experiments revealed a gammarid mortality threshold response to DO at 3 mg L<sup>-1</sup> (Fig. S1). The predictions of the calibrated GUTS model based on our field data for storm and drying events thus follow this threshold, with mortality occurring when DO <3 mg L<sup>-1</sup> (Fig. 6). There was a clear difference in mortality profiles between drying and storm hypoxic events, with a staircase shape for the drying, and a more continuous and abrupt shape for storms. The staircase mortality under drying is due to the marked diel DO oscillations that allow oxidic recovery periods during the day. Hence, the time between the start of hypoxia and the quasi-extinction of the population of individuals (e.g. 95 % dead) is much shorter for storms than for drying events. Specifically, storm events achieved quasi-extinction in less than two days for the three storm events considered, whereas it took at least three days for the drying events, with one drying event not crossing 50 % mortality (Fig. 6b).

During drying, successive mortality events were triggered for successively lower DO thresholds. This is explained by the Individual Tolerance assumption in GUTS model, where the population loses the most sensitive individuals first, but only the most tolerant ones when the stress conditions worsen. This is most apparent for the longer drying event (blue line on Fig. 6b) with a first large event of mortality at day 9 when DO concentrations reach 3 mg L<sup>-1</sup>, followed by a phase without mortality between days 10–15 while DO still fluctuates in the same concentration range. A second event of mortality occurs only when DO <2 mg L<sup>-1</sup>.

## 4. Discussion

### 4.1. Hypoxia is abundant in space and time in headwaters

Hypoxia was temporally common over the growing season across our study area, with a surprisingly even spatial distribution across



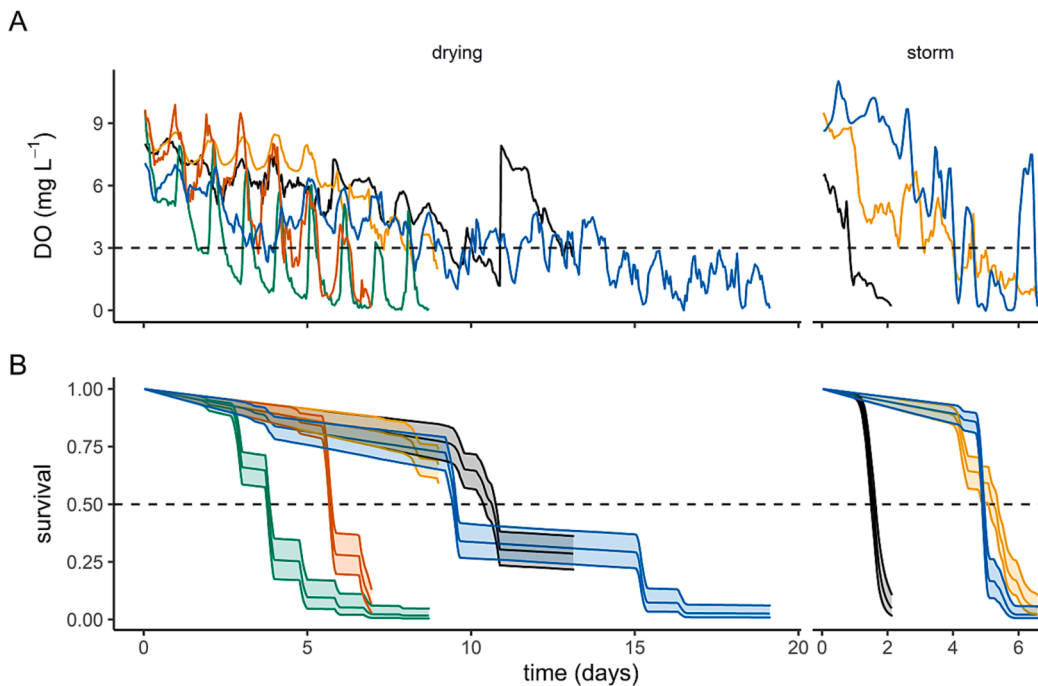


**Fig. 6.** Summary of GUTS model results for gammarid survival under hypoxia driven by drying and storms. A) Time series of DO concentrations for eight different hypoxic events (five drying and three storms), colored by individual event. B) Time series of gammarid survival (1 = 100 % population survives, 0 = complete mortality) with 95 % confidence intervals in shade. Dashed lines indicate hypoxia and 50 % mortality in A and B, respectively. Note different x-axis lengths for storms and drying.

watersheds and Strahler orders. This ran counter to our hypothesis that hypoxia would occur preferentially in the smallest streams (e.g., Strahler order <3), and there was moreover little difference in degree of hypoxia among sites. Equally surprising was that there were marginal differences between night and day hypoxia at the study- or Strahler order-level (cf. Carter et al. 2021), suggesting that when it occurs, it spans full night and day periods. Still, hypoxia was slightly more common in the early evening, suggesting most grab-sample monitoring approaches are underestimating its extent. Spatially, although we sampled Strahler order 3 ( $n = 29$ ) at twice the rate of order 2 ( $n = 14$ ) and five times the rate of order 1 ( $n = 6$ ), normalized hypoxia metrics still indicate parity among these smallest orders with the larger orders 4 ( $n = 21$ ) and 5 ( $n = 8$ ). Although common across Strahler orders, hypoxia occurrence was spatially stochastic and created patches of oxic and hypoxic areas that were separated as a function of local characteristics unquantified here (Fig. S3, Table 3). This is an important nuance to consider when modeling at larger scales: e.g., drying does not uniformly induce hypoxia.

The unexpected commonality of hypoxic conditions in this study supports growing observations of apparent non-eutrophication related hypoxia across watersheds of varying size, climate, geology, and land use (Błaszczak et al., 2019; Carter et al., 2021; Gómez-Gener et al., 2020). Thus, hypoxia may be an overlooked aspect of catchment hydrochemistry, with implications for nutrient processing and community dynamics (Pardo and García, 2016).

#### 4.2. Hydrologic events induce variable hypoxia trajectories

Hypoxia events exhibited distinct characteristics—from initiation to recovery—that depended on hydrologic event type. The most rapid hypoxia trajectories evolved under storm events (Fig. 3a) and rewetting (Fig. 5a). Both storm and rewetting events exhibited dynamic DO changes, which were not explained by several common sense factors such as size of the storm pulse, time since last storm or last rewetting cycle, stream habitat, or Strahler order. However, we note that pools were generally slower to reach hypoxia than runs under rewetting events, likely due to their greater water volume and oxygen mass. Overall, we noted the emergence of several archetypal storm pulse DO behaviors, including no changes (Fig. 3a pool, middle blue line), rapid drops (Fig. 3a, run habitats), a peak of high DO aligning with the storm

peak followed by gradual drawdown to hypoxia (Fig. 3a riffle habitat, middle line), and a gradual drawdown without a peak of high DO (Fig. 3a, riffle, top black line). No change DO archetypes are likely common when instream biological activity is negligible compared to gas exchange. These archetypes are thus mostly relegated to small Strahler orders, where DO signals are driven by low respiration and high gas exchange, and storms do not substantially change the relative influence of either. Point source inflows of low DO or high oxygen-demanding substances may explain the rapid DO drop storm archetype observed here (Dutton et al., 2018). The third archetype of a DO peak followed by drawdown was the most commonly observed in a low-gradient, humid catchment with an order of magnitude higher discharge (Carter et al., 2021), hinting at a common driver. We suggest this could be a hydrologic mechanism.

Storm peaks likely drive high gas exchange, leading to rapid oxygenation, but afterwards we hypothesize that increased soil respiration after storm events (Lee et al., 2004; Sponseller, 2007) entails low DO water to the stream after the storm peak. Soil respiratory processes may reduce the DO in hillslope or nearby riparian groundwater, especially as rising groundwater intercepts greater proportions of soil carbon (Li et al., 2021; McGuire and McDonnell, 2010) as noted in dissolved organic carbon export patterns (e.g., Diamond and Cohen, 2018; Zarnetske et al., 2018). Such soil respiration pulses typically last <48 h (Lee et al., 2004) and would likely arrive in baseflow after the peak, roughly aligning with the timeframe of our observations. Thus, the gradual drawdown aspect of both the third and fourth archetype may be explained by mobilization of “old” water lateral inflows during storm events that push low DO water into the stream channel at a volume that replaces any pre-storm in-channel DO (Brown et al., 1999; Buttle, 1994; Klaus and McDonnell, 2013).

In contrast to storms and rewetting, drying events consistently exhibited a gradual DO drawdown towards hypoxia. These drawdowns were often associated with large diel swings in DO, particularly for pools and runs (Fig. 3a). Such swings would often lead to temporary relief from hypoxia during daylight hours, unless primary productivity and gas exchange were too low to match respiratory demand. There are likely several mechanisms that drive hypoxia under drying. For example, as streams become ahrhic (Gallart et al. 2012), gas exchange decreases leading to dominance of respiration in the DO signal and gradual DO

drawdown. We occasionally observed diel inversion of the common DO signal (i.e., DO maxima at night and minima near noon) for drying pools of smaller streams, suggesting a diel respiration signal driven by temperature. This effect can also occur in larger streams when daily DO replenishment from primary production decreases as producers deplete water column nutrient stocks (Hensley and Cohen 2020). Importantly, it was during drying periods that the stream network as a whole was the most likely to undergo synchronous hypoxia (cf. Diamond et al. 2022), although individual site trajectories towards hypoxia were highly heterogeneous. Dry periods thus compound hydrologic stress on organisms with low oxygen stress, and likely represent critical periods for meta-community development (Sarremejane et al., 2017).

#### 4.3. Hypoxia induced potential mortality of an indicator species

The combination of hypoxia mode, magnitude, and temporal characteristics controlled the extent of organismal mortality or survival. Storm (or rewetting) events induced classic pulse disturbances with rapid mortality, whereas drying was more akin to a stress disturbance with gradual mortality (Fig. 6) (Bender et al., 1984). As such, drying press disturbances may leave possibilities for gammarids to find modes of survival during daytime hypoxia alleviations due to DO increases from primary productivity. This is in contrast to storms, which cause more intense and rapid crashes in DO. Hence, it is not just the presence of hypoxia, but the trajectory into and out of it that likely matters to biota.

We note here that the coupling of seasonal population phenology and hypoxia is likely a strong control of subsequent drops in gammarid densities. For instance, we observed most hypoxia during summer, but population models demonstrate that this is the least sensitive period of gammarid demography to adult mortality (Coulaud et al., 2014), suggesting some inherent population-level resilience. Conversely, while there is limited evidence on embryo or egg response to hypoxia, it seems plausible that these life phases may be more sensitive than the adults tested here, implying major demographic consequences in summer (Geffard et al 2010; Coulaud et al 2014).

Despite our findings of a clear risk of hypoxia-induced mortality events for the gammarid populations, these modeled outcomes need to be supported by empirical studies. For example, additional lab manipulations with variable DO concentrations, and in-situ exposure studies will allow more nuanced study of how DO dynamics affect populations. Moreover, such studies would permit direct testing of the Individual Tolerance approach used in this work. Our choice for using the Individual Tolerance model, which assumes that there are differences in sensitivity among individuals, derives purely from its better fit with the lab data. The hypothesis of the existence of tolerant and sensitive individuals could be tested in the lab by applying, for example, two successive hypoxia events to evaluate if the mortality levels shift at the second event. The likely existence of less sensitive individuals would imply inheritance of genetic fortitude against hypoxia such that future generations may be more tolerant of increasingly lower levels of DO.

#### 4.4. Difficulty predicting hypoxia

We did not find a simple, robust way to predict hypoxic events based on site level habitat, geomorphic, hydrologic, or thermal conditions. These are all relatively easy to measure attributes of streams that are often incorporated as fundamental parts of many stream ecosystem and hydrological models, so seeing no strong predictive power in them presents a challenge for easy modeling of hypoxia in headwaters. Our best model suggests that hypoxia tends to occur under high temperature, low slope, low discharge, and small Strahler order conditions, but this model still had very limited predictive success (67 % true positive rate). These best predictors tend to align with other stream DO work, particularly the small slope (Carter et al., 2021) and low discharge-small Strahler order conditions (Gómez-Gener et al., 2020). Within these

conditions, and under storm event conditions, we did not observe clear predictors of the degree of hypoxia (e.g., hypoxia duration)—we could only assess the likelihood for some level of hypoxia to occur. Hence, there are missing fundamental controls in our array of predictors that can distinguish these hypoxic events. Perhaps the lack of geomorphologic complexity across sites limited the gradient of predictors able to explain the variance in hypoxia, but the diversity of hypoxic trajectories and responses even within a narrow range geographic area suggests the need for alternative hypotheses on hypoxia controls. We surmise that local hydrology—especially lateral inflows, point sources, and hyporheic exchange, which were poorly constrained here—is likely a strong predictor of hypoxia dynamics at the scale of small headwater streams.

#### 4.5. Consistent oxygen drawdown under various conditions

Despite the fact that we observed a range of hypoxic trajectories under storms, drying, and rewetting events, the median rate of drawdown leading to hypoxia was remarkably similar across events and sites—approximately  $1 \text{ mg O}_2 \text{ L}^{-1} \text{ d}^{-1}$ . On the one hand, if hydrologically driven mechanisms dominate, this could indicate an increasing downstream rate of lateral inflow (c.f., Ward et al. 2018). That is, if riparian soil DO is relatively similar along the catchment, increasingly greater lateral flow rates are needed to maintain constant downstream DO drawdowns (by mass conservation). While this may be plausible for some storm events, it would fail to explain drawdown similarities among storms, drying, and rewetting. Alternatively, if in-stream biological mechanisms dominate, that this may imply an increasing downstream network-scale oxygen demand (i.e., “ecosystem respiration” [ $\text{g O}_2 \text{ m}^{-2} \text{ d}^{-1}$ ]). For this pattern to emerge, oxygen demand should increase downstream at roughly the same rate as depth increases (e.g., in proportion to  $d \approx Q^{0.3}$ ; Raymond et al. 2012). This is because depth increases the volume of water and thus the mass of oxygen at a given concentration: mass flux must therefore increase to reduce the concentration by a consistent magnitude at increasing volumes. This downstream increase in demand may only become apparent when the balancing DO controls of primary production and gas exchange are minimal. Indeed, under storm and recession conditions, primary production is often reset to zero due to scouring and turbidity (O'Donnell and Hotchkiss, 2022; Uehlinger, 2000; Uehlinger and Naegeli, 1998) leading to respiration dominance. Under drying conditions, pool formation and low flow reduce gas exchange (Stanley et al., 1997) and reduced replenishment of upstream nutrients for primary production, lead to respiration dominance of the DO signal. Interestingly, previous efforts observed weak-to-no longitudinal pattern of ecosystem respiration in this region, although DO proxies for ecosystem respiration revealed strong downstream increases (Diamond et al., 2021).

The observation of similar DO drawdown under varying conditions is at the very least useful as a rule-of-thumb for managers when wanting to estimate time-until-hypoxia. For instance, assuming typical summer conditions with daily DO minima around  $7 \text{ mg L}^{-1}$ , one could expect the first instances of hypoxia in about four days under drought conditions. Moreover, we observed similar durations of hypoxia (ca. 7-hours) among drying and storm events, implying an additional rule-of-thumb when estimating or modeling hypoxia-induced mortality of sensitive species. Importantly, drying-induced hypoxia is likely to be exacerbated upon rewetting, suggesting a compounded effect of drought on DO quality. Also useful to managers and researchers is that our results demonstrate that low Strahler order streams, despite being historically overlooked for hypoxia, will be the most likely to undergo hypoxia in drought conditions. In other words, these river network capillaries should be hotspots for future investigation of hypoxia and its biological effects.

## 5. Conclusions

We observed regular hypoxic conditions across eight temperature agricultural networks with varying land use, geology, and hydrology. Although common, hypoxia occurrence was spatially stochastic and created patches of oxic and hypoxic reaches. Hypoxia across 78 sites spanning Strahler orders 1–5 was driven by storms, drying, and rewetting, with drying being the dominant mechanism. Models based on our field data indicated that storms and drying events are pulse- and press-disturbances, respectively, whose distinct hypoxia signals induce corresponding mortality profiles in sensitive species. We conclude that the DO trajectory into and out of hypoxia drives mortality patterns with implications for metacommunity structure and development. Despite difficulty in predicting the degree and specific occurrences of hypoxia, we showed that hypoxia is most likely to occur in small, low slope streams, under high temperature and low discharge conditions, but that storm-induced hypoxia is preponderant to higher order streams. Regardless of the hydrologic driver of hypoxia, we observed a remarkably consistent daily drawdown in DO of 1 mg L<sup>-1</sup>, suggesting a downstream increase in oxygen demand, and a useful rule-of-thumb for managers. Overall, we conclude that hypoxia is a regular and increasingly common occurrence in headwater networks with the potential to be a strong control on biogeochemistry and biological communities, meriting its continued study.

## Declaration of Competing Interest

The authors declare that they have no known competing financial interests or personal relationships that could have appeared to influence the work reported in this paper.

## Data availability

Data will be made available on request.

## Acknowledgments

This project was supported by The Loire-Bretagne Water Agency and the Rhône-Méditerranée-Corse Water Agency. JD was also supported by the EUR H2O'Lyons, French ANR-17- EURE-0018 grant. JZ contributions were partially supported by US NSF awards (1846855, 1916567) and a fellowship from the Collegium – Lyon, Institute for Advanced Study. We thank Pierre Martinache and Nicolas Delorme for technical support with lab tests and field work, and Sandrine Charles (UMR 5558 Lyon 1) for her advice on modelling gammarid mortality. We also thank Michèle Gaillet and Paul Courbière for their very kind hospitality to access field sites and to develop experiments on their properties.

## Appendix A. Supplementary data

Supplementary data to this article can be found online at <https://doi.org/10.1016/j.ecolind.2023.109987>.

## References

- Acuña, V., Muñoz, I., Giorgi, A., Omella, M., Sabater, F., Sabater, S., 2005. Drought and postdrought recovery cycles in an intermittent Mediterranean stream: structural and functional aspects. *Journal of the North American Benthological Society* 24, 919–933. <https://doi.org/10.1899/04-078.1>.
- Bastviken, D., Cole, J., Pace, M., Tranvik, L., 2004. Methane emissions from lakes: Dependence of lake characteristics, two regional assessments, and a global estimate. *Global Biogeochemical Cycles* 18. <https://doi.org/10.1029/2004GB002238>.
- Baudrot, V., Veber, P., Gence, G., Charles, S., 2018. Fit Reduced GUTS Models Online: From Theory to Practice. *Integrated Environmental Assessment and Management* 14, 625–630. <https://doi.org/10.1002/ieam.4061>.
- Bender, E.A., Case, T.J., Gilpin, M.E., 1984. Perturbation Experiments in Community Ecology: Theory and Practice. *Ecology* 65, 1–13. <https://doi.org/10.2307/1939452>.
- Benstead, J.P., Leigh, D.S., 2012. An expanded role for river networks. *Nature Geosci* 5, 678–679. <https://doi.org/10.1038/ngeo1593>.
- Bishop, K., Buffam, I., Erlandsson, M., Fölster, J., Laudon, H., Seibert, J., Temnerud, J., 2008. Aqua Incognita: the unknown headwaters. *Hydrol. Process.* 22, 1239–1242. <https://doi.org/10.1002/hyp.7049>.
- Blaszczak, J.R., Delesantro, J.M., Urban, D.L., Doyle, M.W., Bernhardt, E.S., 2019. Scoured or suffocated: Urban stream ecosystems oscillate between hydrologic and dissolved oxygen extremes. *Limnology and Oceanography* 64, 877–894.
- Bond, N., 2022. Hydrostats: Hydrologic Indices for Daily Time Series Data. R package version (2), 9.
- Breitburg, D., Levin, L.A., Oschlies, A., Grégoire, M., Chavez, F.P., Conley, D.J., Garçon, V., Gilbert, D., Gutiérrez, D., Isensee, K., Jacinto, G.S., Limburg, K.E., Montes, I., Naqvi, S.W.A., Pitcher, G.C., Rabalais, N.N., Roman, M.R., Rose, K.A., Seibel, B.A., Telszewski, M., Yasuhara, M., Zhang, J., 2018. Declining oxygen in the global ocean and coastal waters. *Science* 359, eaam7240. <https://doi.org/10.1126/science.aam7240>.
- Brown, V.A., McDonnell, J.J., Burns, D.A., Kendall, C., 1999. The role of event water, a rapid shallow flow component, and catchment size in summer stormflow. *Journal of Hydrology* 217, 171–190. [https://doi.org/10.1016/S0022-1694\(98\)00247-9](https://doi.org/10.1016/S0022-1694(98)00247-9).
- Buttle, J.M., 1994. Isotope hydrograph separations and rapid delivery of pre-event water from drainage basins. *Progress in Physical Geography: Earth and Environment* 18, 16–41. <https://doi.org/10.1177/030913339401800102>.
- Carter, A.M., Blaszczak, J.R., Heffernan, J.B., Bernhardt, E.S., 2021. Hypoxia dynamics and spatial distribution in a low gradient river. *Limnology and Oceanography*.
- Charles, S., Veber, P., Delignette-Muller, M.L., 2018. MOSAIC: a web-interface for statistical analyses in ecotoxicology. *Environ Sci Pollut Res* 25, 11295–11302. <https://doi.org/10.1007/s11356-017-9809-4>.
- Chaumot, A., Geffard, O., Armengaud, J., Maltby, L., 2015. Chapter 11 - Gammarids as Reference Species for Freshwater Monitoring. In: Amiard-Triquet, C., Amiard, J.-C., Mouneyrac, C. (Eds.), *Aquatic Ecotoxicology*. Academic Press, pp. 253–280. <https://doi.org/10.1016/B978-0-12-800949-9.00011-5>.
- Coulaud, R., Geffard, O., Coquillat, A., Quéau, H., Charles, S., Chaumot, A., 2014. Ecological Modeling for the Extrapolation of Ecotoxicological Effects Measured during in Situ Assays in Gammarus. *Environ. Sci. Technol.* 48, 6428–6436. <https://doi.org/10.1021/es501126g>.
- Dai, A., 2013. Increasing drought under global warming in observations and models. *Nature Clim Change* 3, 52–58. <https://doi.org/10.1038/nclimate1633>.
- Diamond, J.S., Bernal, S., Boukra, A., Cohen, M.J., Lewis, D., Masson, M., Moatar, F., Pinay, G., 2021. Stream network variation in dissolved oxygen: Metabolism proxies and biogeochemical controls. *Ecological Indicators* 131, 108233. <https://doi.org/10.1016/j.ecolind.2021.108233>.
- Diamond, J.S., Cohen, M.J., 2018. Complex patterns of catchment solute–discharge relationships for coastal plain rivers. *Hydrological Processes* 32, 388–401. <https://doi.org/10.1002/hyp.11424>.
- Diamond, J.S., Pinay, G., Bernal, S., Cohen, M.J., Lewis, D., Lupon, A., Zarnetske, J., Moatar, F., 2022. Light and hydrologic connectivity drive dissolved oxygen synchrony in stream networks. *Limnology and Oceanography* 00, 1–14. <https://doi.org/10.1002/lno.12271>.
- Dutton, C.L., Subalusky, A.L., Hamilton, S.K., Rosi, E.J., Post, D.M., 2018. Organic matter loading by hippopotami causes subsidy overload resulting in downstream hypoxia and fish kills. *Nat Commun* 9, 1951. <https://doi.org/10.1038/s41467-018-04391-6>.
- Elliott, J., Deryng, D., Müller, C., Frieler, K., Konzmann, M., Gerten, D., Glotter, M., Flörke, M., Wada, Y., Best, N., Eisner, S., Fekete, B.M., Folberth, C., Foster, I., Gosling, S.N., Haddeland, I., Khabarov, N., Ludwig, F., Masaki, Y., Olin, S., Rosenzweig, C., Ruane, A.C., Satoh, Y., Schmid, E., Stacke, T., Tang, Q., Wisser, D., 2014. Constraints and potentials of future irrigation water availability on agricultural production under climate change. *Proceedings of the National Academy of Sciences* 111, 3239–3244. <https://doi.org/10.1073/pnas.1222474110>.
- Gallart, F., Prat, N., García-Roger, E.M., Latron, J., Rieradevall, M., Llorens, P., Barberá, G.G., Brito, D., De Girolamo, A.M., Lo Porto, A., Buffagni, A., Erba, S., Neves, R., Nikolaidis, N.P., Perrin, J.L., Querner, E.P., Quinóner, J.M., Tournoud, M.G., Tzoraki, O., Skoulikidis, N., Gómez, R., Sánchez-Montoya, M.M., Froebrich, J., 2012. A novel approach to analysing the regimes of temporary streams in relation to their controls on the composition and structure of aquatic biota. *Hydrology and Earth System Sciences* 16, 3165–3182. <https://doi.org/10.5194/hess-16-3165-2012>.
- Garvey, J.E., Whiles, M.R., Streicher, D., 2007. A hierarchical model for oxygen dynamics in streams. *Canadian Journal of Fisheries and Aquatic Sciences* 64, 1816–1827.
- Gnouma, R., 2006. Aide à la calibration d'un modèle hydrologique distribué au moyen d'une analyse des processus hydrologiques: application au bassin versant de l'Yzeron. Thèse de doctorat, INSA Lyon.
- Godsey, S.E., Kirchner, J.W., 2014. Dynamic, discontinuous stream networks: hydrologically driven variations in active drainage density, flowing channels and stream order. *Hydrological Processes* 28, 5791–5803.
- Gómez-Gener, L., Lupon, A., Laudon, H., Sponseller, R.A., 2020. Drought alters the biogeochemistry of boreal stream networks. *Nat Commun* 11, 1795. <https://doi.org/10.1038/s41467-020-15496-2>.
- Gouty, V., Liger, L., Ahrouh, S., Bonneau, C., Carlier, N., Chaumot, A., Coquery, M., Dabrin, A., Margoum, C., Pesce, S., 2021. Ardières-Morcille in the Beaujolais, France: A research catchment dedicated to study of the transport and impacts of diffuse agricultural pollution in rivers. *Hydrological Processes* 35, e14384.
- Hensley, R.T., Cohen, M.J., 2020. Nitrate depletion dynamics and primary production in riverine benthic chambers. *Freshwater. Science* 39 (1), 169–182. <https://doi.org/10.1086/707650>.
- Hervant, F., Mathieu, J., 1995. Ventilatory and locomotory activities in anoxia and subsequent recovery of epigeal and hypogean crustaceans. *Comptes rendus de l'Académie des sciences. Série III, Sciences de la vie* 318, 585–592.

- Jager, T., Albert, C., Preuss, T.G., Ashauer, R., 2011. General Unified Threshold Model of Survival - a Toxicokinetic-Toxicodynamic Framework for Ecotoxicology. *Environ. Sci. Technol.* 45, 2529–2540. <https://doi.org/10.1021/es103092a>.
- Jenny, J.-P., Francus, P., Normandeau, A., Lapointe, F., Perga, M.-E., Ojala, A., Schimmelmann, A., Zolitschka, B., 2016. Global spread of hypoxia in freshwater ecosystems during the last three centuries is caused by rising local human pressure. *Global Change Biology* 22, 1481–1489. <https://doi.org/10.1111/gcb.13193>.
- Kerr, J.L., Baldwin, D.S., Whitworth, K.L., 2013. Options for managing hypoxic blackwater events in river systems: A review. *Journal of Environmental Management* 114, 139–147. <https://doi.org/10.1016/j.jenvman.2012.10.013>.
- Klaus, J., McDonnell, J.J., 2013. Hydrograph separation using stable isotopes: Review and evaluation. *Journal of Hydrology* 505, 47–64. <https://doi.org/10.1016/j.jhydrol.2013.09.006>.
- Kunz, P.Y., Kienle, C., Gerhardt, A., 2010. Gammarus spp. in Aquatic Ecotoxicology and Water Quality Assessment: Toward Integrated Multilevel Tests. In: Whitacre, D.M. (Ed.), *Reviews of Environmental Contamination and Toxicology Volume 205, Reviews of Environmental Contamination and Toxicology*. Springer, New York, NY, pp. 1–76. [https://doi.org/10.1007/978-1-4419-5623-1\\_1](https://doi.org/10.1007/978-1-4419-5623-1_1).
- Lee, X., Wu, H.-J., Sigler, J., Oishi, C., Siccama, T., 2004. Rapid and transient response of soil respiration to rain. *Global Change Biology* 10, 1017–1026.
- Li, L., Sullivan, P.L., Benettin, P., Cirpka, O.A., Bishop, K., Brantley, S.L., Knapp, J.L.A., van Meerveld, I., Rinaldo, A., Seibert, J., Wen, H., Kirchner, J.W., 2021. Toward catchment hydro-biogeochemical theories. *WIREs. Water* 8, e1495.
- Lunardon, N., Menardi, G., Torelli, N., 2014. ROSE: a Package for Binary Imbalanced Learning. *R Journal* 6, 82–92.
- Macneil, C., Dick, J.T.A., Elwood, R.W., 1997. The trophic ecology of freshwater Gammarus spp. (Crustacea: Amphipoda): problems and perspectives concerning the functional feeding group concept. *Biol. Rev. Cambridge Phil. Soc.* 72, 349–364. <https://doi.org/10.1111/j.1469-185X.1997.tb00017.x>.
- Mallin, M.A., Johnson, V.L., Ensign, S.H., MacPherson, T.A., 2006. Factors contributing to hypoxia in rivers, lakes, and streams. *Limnology and Oceanography* 51, 690–701. [https://doi.org/10.4319/lo.2006.51.1\\_part\\_2.0690](https://doi.org/10.4319/lo.2006.51.1_part_2.0690).
- Maltby, L., 1995. Sensitivity of the crustaceans *Gammarus pulex* (L.) and *Asellus aquaticus* (L.) to short-term exposure to hypoxia and unionized ammonia: Observations and possible mechanisms. *Water Research* 29, 781–787. [https://doi.org/10.1016/0043-1354\(94\)00231-U](https://doi.org/10.1016/0043-1354(94)00231-U).
- McConnell, J.B., 1980. Impact of Urban Storm Runoff on Stream Quality Near Atlanta, Georgia. Municipal Environmental Research Laboratory, Office of Research and Development. U.S. Environmental Protection Agency.
- McFadden, D., 1987. Regression-based specification tests for the multinomial logit model. *Journal of econometrics* 34, 63–82.
- McGuire, K.J., McDonnell, J.J., 2010. Hydrological connectivity of hillslopes and streams: Characteristic time scales and nonlinearities. *Water Resources Research* 46. <https://doi.org/10.1029/2010WR009341>.
- Meijering, M.P.D., 1991. Lack of oxygen and low pH as limiting factors for *Gammarus* in Hessian brooks and rivers. *Hydrobiologia* 223, 159–169. <https://doi.org/10.1007/BF00047637>.
- Ministère chargé de l'écologie, 2019. Guide technique: relatif à l'évaluation de l'état des eaux de surface continentales (cours d'eau, canaux, plans d'eau).
- Montuelle, B., Dorigo, U., Bérard, A., Volat, B., Bouchez, A., Tlili, A., Gouy, V., Pesce, S., 2010. The periphyton as a multimetric bioindicator for assessing the impact of land use on rivers: an overview of the Ardères-Morcille experimental watershed (France). *Hydrobiologia* 657, 123–141. <https://doi.org/10.1007/s10750-010-0105-2>.
- NSTC, 2003. An assessment of coastal hypoxia and eutrophication in US waters. National Science and Technology Council, Committee on Environment and Natural Resources.
- O'Donnell, B., Hotchkiss, E.R., 2022. Resistance and resilience of stream metabolism to high flow disturbances. *Biogeosciences* 19, 1111–1134. <https://doi.org/10.5194/bg-19-1111-2022>.
- Ockleford, C., Adriaanse, P., Berny, P., Brock, T., Duquesne, S., Grilli, S., Hernandez-Jerez, A.F., Bennekou, S.H., Klein, M., Kuhl, T., Laskowski, R., Machera, K., Pelkonen, O., Pieper, S., Smith, R.H., Stemmer, M., Sundh, I., Tiktak, A., Topping, C. J., Wolterink, G., Cedergreen, N., Charles, S., Focks, A., Reed, M., Arena, M., Ippolito, A., Byers, H., Teodorovic, I., 2018. Scientific Opinion on the state of the art of Toxicokinetic/ Toxicodynamic (TKTD) effect models for regulatory risk assessment of pesticides for aquatic organisms. *EFSA Journal* 16, e05377.
- Pardo, I., García, L., 2016. Water abstraction in small lowland streams: Unforeseen hypoxia and anoxia effects. *Science of The Total Environment* 568, 226–235. <https://doi.org/10.1016/j.scitotenv.2016.05.218>.
- Penn, C.A., Bearup, L.A., Maxwell, R.M., Clow, D.M., 2016. Numerical experiments to explain multiscale hydrological responses to mountain pine beetle tree mortality in a headwater watershed, *Water Resour. Res.* 52, 3143–3161. <https://doi.org/10.1002/2015WR018300>.
- Rabalais, N.N., Díaz, R.J., Levin, L.A., Turner, R.E., Gilbert, D., Zhang, J., 2010. Dynamics and distribution of natural and human-caused hypoxia. *Biogeosciences* 7, 585–619. <https://doi.org/10.5194/bg-7-585-2010>.
- Recoura-Massaquant, R., Martinache, P., Delorme, N., Chaumot, A., 2022. Experimental test of *Gammarus fossarum* sensitivity to hypoxic stress (No. Recherche Data Gouy, V1). INRAE.
- Rode, M., Wade, A.J., Cohen, M.J., Hensley, R.T., Bowes, M.J., Kirchner, J.W., Arhonditsis, G.B., Jordan, P., Kronvang, B., Halliday, S.J., Skeffington, R.A., Rozemeijer, J.C., Aubert, A.H., Rinke, K., Jomaa, S., 2016. Sensors in the Stream: The High-Frequency Wave of the Present. *Environ. Sci. Technol.* 50, 10297–10307. <https://doi.org/10.1021/acs.est.6b02155>.
- Saari, G.N., Wang, Z., Brooks, B.W., 2018. Revisiting inland hypoxia: diverse exceedances of dissolved oxygen thresholds for freshwater aquatic life. *Environ Sci Pollut Res* 25, 3139–3150. <https://doi.org/10.1007/s11356-017-8908-6>.
- Samaniego, L., Thober, S., Kumar, R., Wanders, N., Rakovec, O., Pan, M., Zink, M., Sheffield, J., Wood, E.F., Marx, A., 2018. Anthropogenic warming exacerbates European soil moisture droughts. *Nature Clim Change* 8, 421–426. <https://doi.org/10.1038/s41558-018-0138-5>.
- Sarremejane, R., Cañedo-Argüelles, M., Prat, N., Mykrä, H., Muotka, T., Bonada, N., 2017. Do metacommunities vary through time? Intermittent rivers as model systems. *Journal of Biogeography* 44, 2752–2763. <https://doi.org/10.1111/jbi.13077>.
- Saup, C.M., Williams, H.K., Rodríguez-Freire, L.M., Cerrato, J.D., Johnston, M.J., Wilkins, M., 2017. Anoxia stimulates microbially catalyzed metal release from Animas River sediments. *Environmental Science: Processes & Impacts* 19, 578–585. <https://doi.org/10.1039/C7EM00036G>.
- Smith, V.H., Schindler, D.W., 2009. Eutrophication science: where do we go from here? *Trends in Ecology & Evolution* 24, 201–207. <https://doi.org/10.1016/j.tree.2008.11.009>.
- Sponseller, R.A., 2007. Precipitation pulses and soil CO<sub>2</sub> flux in a Sonoran Desert ecosystem. *Global Change Biology* 13, 426–436.
- Stanley, E.H., Fisher, S.G., Grimm, N.B., 1997. Ecosystem Expansion and Contraction in Streams. *BioScience* 47, 427–435. <https://doi.org/10.2307/1313058>.
- Strahler, A.N., 1957. Quantitative analysis of watershed geomorphology. *Eos, Transactions American Geophysical Union*. 38, 913–920.
- Therneau, T., Atkinson, B., 2022. rpart: Recursive Partitioning and Regression Trees.
- Tramer, E.J., 1977. Catastrophic Mortality of Stream Fishes Trapped in Shrinking Pools. *The American Midland Naturalist* 97, 469–478. <https://doi.org/10.2307/2425110>.
- Uehlinger, U., 2000. Resistance and resilience of ecosystem metabolism in a flood-prone river system. *Freshwater Biology* 45, 319–332. <https://doi.org/10.1111/j.1365-2427.2000.00620.x>.
- Uehlinger, U., Naegeli, M.W., 1998. Ecosystem Metabolism, Disturbance, and Stability in a Prealpine Gravel Bed River. *Journal of the North American Benthological Society* 17, 165–178. <https://doi.org/10.2307/1467960>.
- Vannote, R.L., Minshall, G.W., Cummins, K.W., Sedell, J.R., Cushing, C.E., 1980. The River Continuum Concept. *Can. J. Fish. Aquat. Sci.* 37, 130–137. <https://doi.org/10.1139/f80-017>.
- Ward, A.S., Schmadel, N.M., Wondzell, S.M., 2018. Simulation of dynamic expansion, contraction, and connectivity in a mountain stream network. *Advances in Water Resources* 114, 64–82. <https://doi.org/10.1016/j.advwatres.2018.01.018>.
- Whitworth, K.L., Baldwin, D.S., Kerr, J.L., 2012. Drought, floods and water quality: Drivers of a severe hypoxic blackwater event in a major river system (the southern Murray-Darling Basin, Australia). *Journal of Hydrology* 450–451, 190–198. <https://doi.org/10.1016/j.jhydrol.2012.04.057>.
- Zarnetske, J.P., Bouda, M., Abbott, B.W., Saiers, J., Raymond, P.A., 2018. Generality of Hydrologic Transport Limitation of Watershed Organic Carbon Flux Across Ecoregions of the United States. *Geophysical Research Letters* 45, 11702–11711. <https://doi.org/10.1029/2018GL080005>.
- Zimmer, M.A., Kaiser, K.E., Blaszczyk, J.R., Zipper, S.C., Hammond, J.C., Fritz, K.M., Costigan, K.H., Hosen, J., Godsey, S.E., Allen, G.H., Kampf, S., Burrows, R.M., Krabbenhoft, C.A., Dodds, W., Hale, R., Olden, J.D., Shanafield, M., DelVecchia, A. G., Ward, A.S., Mims, M.C., Datry, T., Bogan, M.T., Boersma, K.S., Busch, M.H., Jones, C.N., Burgin, A.J., Allen, D.C., 2020. Zero or not? Causes and consequences of zero-flow stream gage readings. *WIREs Water* 7, e1436.